

A Novel Energetic Perchlorate Amine Salt: Synthesis, Properties, and Density Functional Theory Calculation

Peng Ma, Yong Pan, Juncheng Jiang & Shunguan Zhu

To cite this article: Peng Ma, Yong Pan, Juncheng Jiang & Shunguan Zhu (2017): A Novel Energetic Perchlorate Amine Salt: Synthesis, Properties, and Density Functional Theory Calculation, Journal of Energetic Materials, DOI: [10.1080/07370652.2016.1269851](https://doi.org/10.1080/07370652.2016.1269851)

To link to this article: <http://dx.doi.org/10.1080/07370652.2016.1269851>



Published online: 04 Jan 2017.



Submit your article to this journal [↗](#)



View related articles [↗](#)



View Crossmark data [↗](#)

A Novel Energetic Perchlorate Amine Salt: Synthesis, Properties, and Density Functional Theory Calculation

Peng Ma^a, Yong Pan^a, Juncheng Jiang^a, and Shunguan Zhu^b

^aJiangsu Key Laboratory of Hazardous Chemicals Safety and Control, College of Safety Science and Engineering, Nanjing Tech University, Nanjing, China; ^bSchool of Chemical Engineering, Nanjing University of Science and Technology, Nanjing, China

ABSTRACT

A novel explosive, ethylenediamine triethylenediamine tetraperchlorate (ETT), was synthesized by a rapid “one-pot” method. The molecular and crystal structures of ETT were determined by X-ray diffraction (XRD) and Fourier transformed infrared (FTIR) spectroscopy. The purity of the ETT was characterized by hydrogen nuclear magnetic resonance (H-NMR) spectra and elemental analysis (EA). The chemical and physical properties of the co-crystal ETT were further explored including impact sensitivity, velocity of detonation, and thermal behavior. The impact sensitivity of the ETT ($h_{50\%} = 9.50$ cm) is much lower than that of its components, ethylenediamine diperchlorate (ED) ($h_{50\%} = 5.60$ cm) and triethylenediamine diperchlorate (TD) ($h_{50\%} = 2.10$ cm). The measured detonation velocity is 8956 m/s ($\rho = 1.873$ g/cm³), which is much higher than that of TNT (6900 m/s) or RDX (8350 m/s). The co-crystal ETT shows a unique thermal behavior with a decomposition peak temperature at 365 °C. Band structure and density of states (DOS) of the ETT were confirmed by the CASTEP code. The first-principles tight-binding method within the general gradient approximation (GGA) was employed to study the electronic band structure as well as the DOS and Fermi energy. Hirshfeld surfaces were applied to analyze the intermolecular interactions in the co-crystal, and the results showed that weak interaction was dominantly mediated by H ... O hydrogen bond. By analyzing the bond length at different temperatures, N-H covalent bond is the trigger bond for the ETT.



KEYWORDS

DFT calculation; ethylenediamine triethylenediamine tetraperchlorate; explosion properties; structure analysis

Introduction

Energetic materials are a class of compounds with significant chemical energy stored in their molecular structures, which are widely used in both military and civil engineering (Badgular et al. 2008; Dippold, Izsák, and Klapötke 2013; Rice, Hare, and Byrd 2007; Xue et al. 2005). In order to improve the performance, such as detonation velocity, sensitivity, and so on, of energetic materials, quite a lot of efforts have been made either by synthesizing new types of energetic materials with desired properties (Yin, Parrish, and Shreeve 2015; Ghule 2013), or using traditional methods such as addition of insensitive compounds. However, it is still an obstacle to develop such materials with both high detonation velocity and low sensitivity (Zhang et al. 2013; van der Heijden et al. 2004; Sikder and Sikder, 2004). Currently, co-crystallization technology provides a new way to obtain high energy density materials with excellent performance (Lin et al. 2013a; Guo et al. 2013; Shen et al. 2011).

Co-crystallization method has been extensively used in the field of pharmaceutical chemistry, due to the advantage of combination of two or more components together through weak interactions, like hydrogen bonds, π stacking, salt bridge, and van der Waals force interactions, without

CONTACT Peng Ma  mpccvt@163.com  Jiangsu Key Laboratory of Hazardous Chemicals Safety and Control, College of Safety Science and Engineering, Nanjing Tech University, Nanjing 210009, China.

Color versions of one or more of the figures in the article can be found online at www.tandfonline.com/uegm.

destroying the chemical structure itself (Remenar et al. 2003; Weyna et al. 2009). Therefore, co-crystallization technology can also be employed to modify the performance of energetic materials (Zhang and Shreeve 2016), such as the energy and sensitivity (Millar et al. 2012; Zhang et al. 2014). Using this method, Matzger et al. (Landenberger and Matzger 2010; Bolton et al. 2011; Landenberger and Matzger 2012; Bolton and Matzger 2012) and Zhu et al. (Lin et al. 2013b; Lin et al. 2013c; Lin et al. 2013d; Lin et al. 2013e) have made great contribution to the field of energetic materials whereby many co-crystal energetic materials have been synthesized with excellent performance such as higher density, better thermal stability, and so on.

So far, nearly all the reported co-crystal energetic materials (CoEMs) are organic compounds, such as CL-20/HMX (Landenberger, Bolton and Matzger 2013) and CL-20/TNT (Guo et al. 2015), since they are prone to form of hydrogen bonds. In addition, most of the CoEMs are only prepared in the laboratory scale, which limits their wide application, because of their low yield. The inorganic compounds can be synthesized with high yield in the large scale as well as the availability and low cost for the raw materials. In addition, plenty of hydrogen bonds in amine perchlorate compounds indicate the feasibility of preparation of the inorganic-organic co-crystals. Scientists from all over the world have done very useful research on the synthesis of CoEMs (Landenberger et al., 2013; Bolton and Matzger 2011; Guo et al. 2015; Landenberger and Matzger 2012). The traditional synthesis route of CoEMs can be divided into two steps: the first step is to get the components (such as CL-20 and TNT), and the next step is the co-crystallization. Using this way to synthesize ethylenediamine triethylenediamine tetraperchlorate (ETT), the components of ETT should be prepared first. Here, we introduce a new “one-pot” synthesis method, which simplifies the two-stage method to a one-stage method: the starting materials were charged in one reactor, and when the reaction finished, the co-crystal formed.

A new type of co-crystal energetic material, ethylenediamine triethylenediamine tetraperchlorate (ETT), was synthesized using the “one-pot” method. X-ray crystallographic measurements were performed on the ETT. In addition, the ETT was characterized using infrared and EA as well as H-NMR spectroscopy. The sensitivity and thermal decomposition data were obtained experimentally. Density functional theory (DFT) calculations were employed to elucidate the relationship between hydrostatic pressure and crystal structure.

Experimental procedure

Sample preparation

ETT is an energetic material that tends to explode under certain conditions. Appropriate safety precautions, such as safety glasses, face shields, and ear plugs should be used. The sample used in this work was prepared in the following procedure: 4.5 g of ethylenediamine and 9.0 g of triethylenediamine were added into a reactor with 60-mL distilled water. The solution was kept with mechanical stirring. 36 g of perchlorate acid was then added dropwise to the glass reactor. The addition of reactant resulted in a strongly exothermic reaction, leading to an increase in the temperature of contents. Notably, the temperature should be controlled below 70 °C, otherwise a higher temperature could destroy the product and affect the quality of the product. The solution was continuously stirred for 30 min after the reaction finished. It was naturally cooled to 25 °C and then left to stand for 0.5h until a white precipitate was formed. When the precipitate was obtained, the reaction flask was digested at room temperature with stirring until the white crystal of ETT was obtained. Using the novel “one-pot” method, a yield of 20 g ETT was obtained within 2 h in laboratory scale from raw materials ethylenediamine, triethylenediamine, and perchlorate acid.

Characterization and calculation

Structure and component of the ETT were characterized by XRD and FTIR spectroscopy. XRD was performed using a four circle CAD4/PC equipped with graphite-monochromatized Mo K α radiation

($\lambda = 0.71074 \text{ \AA}$). The crystal of ETT, having the edges of $0.30 \text{ mm} \times 0.20 \text{ mm} \times 0.20 \text{ mm}$, was used to collect the intensity data at $293(2) \text{ K}$. XRD results indicate that the empirical formula of ETT is $\text{C}_8\text{H}_{14}\text{O}_{16}\text{N}_4\text{Cl}_4$. FTIR results of ETT were recorded by a Bruker Equinox 55 spectrometer (Equinox 55 Bruker Banner Lane, Coventry, Germany). Samples for FTIR were prepared with KBr and pressed to form disks. The purity of the ETT was characterized by H-NMR spectra and EA. ^1H -NMR spectra of the ETT was recorded in D_2O at room temperature with a DPX300 (Bruker Physik AG, Germany). EA of the ETT was tested using elemental vario MICRO cube (Germany).

The weak interactions in co-crystal were analyzed by Hirshfeld surfaces. Hirshfeld surfaces were mapped using the normalized contact distance (d_{norm}), which is calculated using the following equation:

$$d_{\text{norm}} = \frac{d_i - r_i^{\text{vdw}}}{r_i^{\text{vdw}}} + \frac{d_e - r_e^{\text{vdw}}}{r_e^{\text{vdw}}}$$

Where d_{norm} is determined by d_i and d_e , the distances from the surface to the nearest atom interior and exterior to the surfaces, respectively, and the van der Waals (vdW) radii of atoms. Hirshfeld surface analysis and the associated two dimensional (2D) fingerprint plots of the ETT were performed using the Crystal Explorer 3.1 (Wolff et al. 2012) software. A Hirshfeld surface is composed of lots of points, and each point can provide information about related contact distances from it.

First-principle calculation based on DFT is now employed in the field of co-crystal explosives. DFT calculations are performed using the CASTEP package (Segall et al. 2002). The package is an ab initio quantum mechanics codes based on DFT. Geometry optimization was carried out using the Broyden—Fletcher—Goldfarb -Shanno (BFGS) method (Fischer and Almlof 1992). For this calculation, the kinetic cutoff energy of 600 eV and a K -point mesh of $2 \times 2 \times 1$ in the Brillouin zone were employed. Interactions between electrons and core ions are described by ultrasoft pseudopotentials (Vanderbilt 1990), and the electronic exchange-correlation was treated with a generalized gradient approximation (GGA) of the Perdew—Burke—Ernzerhof (PBE) functional (Perdew, Burke, and Ernzerhof 1996).

Results and discussion

Structure characterization

The organic cation and the inorganic anion are held together by hydrogen bonds N-H ... O as shown in Figure 1 and Table 1. Specially, hydrogen from methylamine could form three different hydrogen bonds, which is called a trigeminal-type hydrogen bond as shown in Figure 2. The asymmetric unit of ETT is shown in Figure 2, which consists of ED and TD.

Infrared, NMR spectrum, and EA analysis

The obtained ETT exhibited characteristic absorption bands, shown in Figure 3, of N–H stretching vibrations of amine groups at 3435 cm^{-1} , C–H stretching vibrations at $3186, 3054, 3013, 2933,$ and 2937 cm^{-1} , and Cl–H bending vibrations at 2595 and 2551 cm^{-1} .

^1H -NMR and EA were used to test the purity of the ETT. According to ^1H -NMR spectra of ETT shown in Figure 4, it can be seen that the ratio of hydrogen around position 3.2 and 3.6 ppm on chemical shift is 3:1 (12.00: 4.02), which is consistent with the ratio in ethylenediamine and triethylenediamine.

The theoretical EA values of ETT are C (17.02%), H (2.48%), Cl (25.18%), N (9.93%), and O (45.39%), respectively, and the experimental results are C (16.17%), H (2.48%), Cl (26.03%), N (9.09%), and O (46.23%), respectively, meaning that the composites of the obtained product match the theoretical results very well. Hence, both the EA and NMR results imply high purity of the ETT.

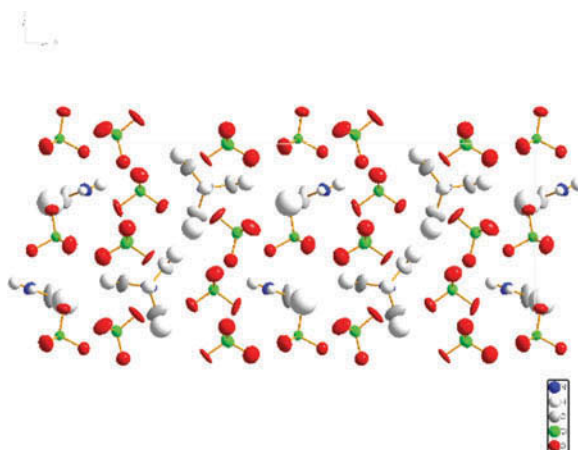


Figure 1. A view of crystal packing of ETT.

Table 1. Intermolecular interaction distances (Å) and angles (deg) of ETT.

Donor-H ... Acceptor	D-H (Å)	H ... A (Å)	D ... A (Å)	D-H ... A (°)
N(1)-H(1A)...O(3)	1.048	2.268	3.158	141.8
N(1)-H(1A)...O(4)	1.048	2.266	3.159	141.3
N(1)-H(1A) ...O(18)	1.048	2.258	3.150	141.8
N(2)-H(2A) ...O(2)	1.049	2.260	3.159	121.9
N(2)-H(2A) ...O(7)	1.049	2.186	3.150	120.3
N(2)-H(2A) ...O(10)	1.049	2.304	2.988	112.0

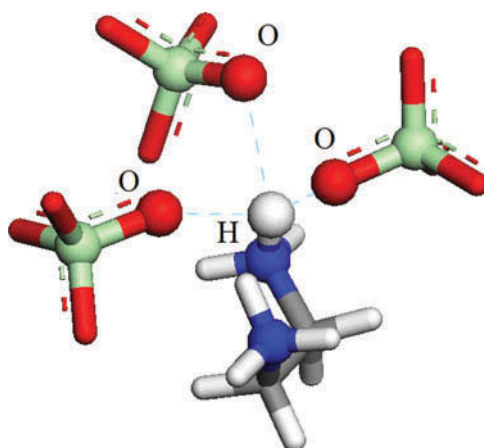


Figure 2. Trigeminal-type hydrogen bond of ETT.

Performance test

Impact sensitivity of the ETT was measured using a Kast drop hammer apparatus with a 10-kg drop hammer. 30 ± 0.05 mg samples were struck with the free-falling drop hammer dropped from variable heights. The sensitivity of ED and TD, components of the ETT, are presented in Table 2.

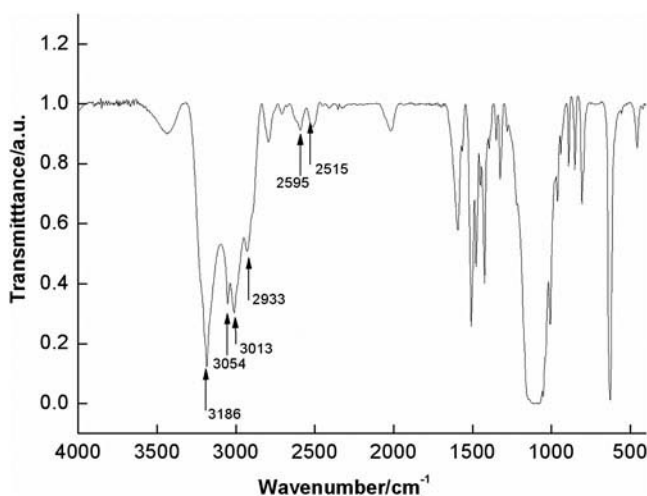


Figure 3. Infrared spectrum of ETT.

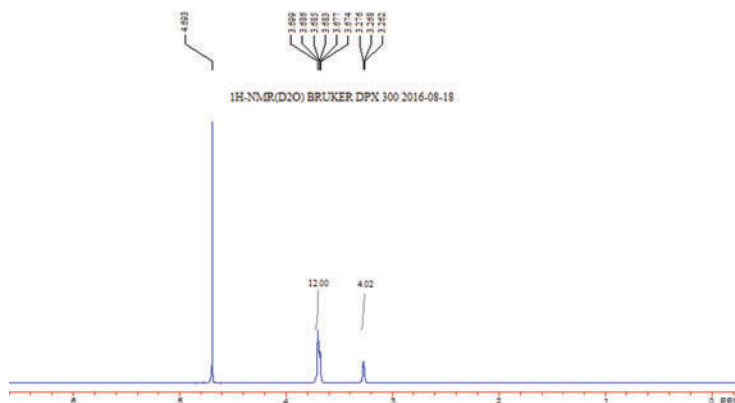


Figure 4. ^1H NMR spectra of ETT (300 MHz, D_2O , TMS).

Table 2. Impact sensitivity of ETT, ED, TD, PETN, and TNT.

Sample	Drop height (cm)
ETT	9.50
PETN	4.43
ED	5.60
TD	2.10
TNT	20.03

Based on the results, the impact sensitivity of the ETT ($h_{50\%} = 9.5$ cm) is nearly 2 times higher than that of Pentaerythritol Tetranitrate (PETN) ($h_{50\%} = 4.4$ cm), which means that the ETT is much safer than PETN. Drop tests reveal identical $h_{50\%}$ values for ED and TD, the components of ETT, are 5.6 and 2.1 cm, respectively, indicating that the two components are more sensitive than the ETT. It is previously reported (Bolton et al. 2012) that the sensitivities of co-crystal would fall between those of their components, and a true synergy is found here as co-crystallization could reduce the sensitivities dramatically. This may be caused by different crystal structures. In addition, we found that crystal structure of the ETT was greatly affected by hydrogen bond. The trigeminal-type

Table 3. Measured VoD of ETT, TNT, RDX, and HMX.

Sample	Density (g/cm ³)	VoD (m/s)
ETT	1.873	8956
TNT	1.620	6900
RDX	1.700	8350
HMX	1.890	9110

Table 4. Heat of formation of ETT compared with TNT, RDX, and PETN.

	ΔH_f (kJ·mol ⁻¹)
ETT	563
TNT	-67
RDX	92
PETN	-407

hydrogen bonds in the ETT could be a significant stabilizing force, which induces that an energetic-energetic co-crystal could reduce the sensitivity. The $h_{50\%}$ value of the ETT is much lower than that of the TNT, exhibiting more sensitivity than TNT. Therefore, the ETT could be used as both a primary and secondary explosive.

Detonation velocity is a critical property to evaluate the performance of energetic materials. The detonation velocities (VoD) of ETT, RDX, HMX, and TNT were tested by a ZBS-10A100 MHz intelligent ten segments detonation velocity measuring instrument at room temperature shown in Table 3.

According to the results presented in Table 3, the VoD of the ETT (8956 m/s) is much higher than that of the TNT (6900 m/s) and RDX (8350 m/s), but still a little lower than that of HMX (9110 m/s). Density has an important influence on VoD, namely the higher density of energetic materials, which means enhanced VoD. This may be explained by that the co-crystal ETT has lower density compared to HMX.

The ETT exhibits positive heat of formation shown in Table 4 calculated using the atomization energy method.

Thermal analysis

The thermal decomposition of the ETT was investigated by differential scanning calorimetry (DSC) (blue curve) and thermogravimetric (TG) (green curve) analyses (see Figure 5). The DSC trace of ETT shows a strong exothermic peak at 365 °C, which is caused by the decomposition of the ETT, higher than the peaks of HMX (285 °C), TNT (210 °C) and HNIW (245–249 °C) (Anniyappan et al. 2015). In addition, the TG curve of ETT shows only one mass loss step, appearing in the temperature range of 350–375 °C, mainly attributed to the intensive thermal decomposition of the ETT.

Theoretical analysis of ETT

In the ETT, hydrogen bonds appear to be the major contributors to the ligands of ethylenediamine and triethylenediamine. In order to confirm the feasibility of the Local Density Approximate (LDA) and GGA methods for the ETT, we compared the calculation results with the experimental data presented in Table 5. Based on comparison with experimental data, the volume obtained by LDA and GGA method is lower by 4% and 3%, separately. Also for the lattice parameters, GGA method is much closer to experimental data. Overall, the standard DFT method GGA reproduces well the ground state structure, and GGA method having a better concordance with experimental results will be employed to calculate other properties.

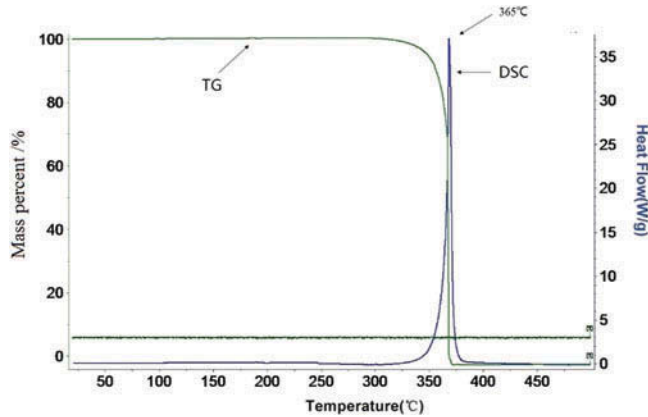


Figure 5. DSC and TG curves of ETT.

Table 5. Comparison of calculated lattice parameters (a , c , and V) of ETT using two DFT methods LDA and GGA with experimental data.

Axis	LDA	GGA	Exp
A (Å)	7.89	7.92	8.103
b (Å)	24.932	24.788	24.725
c (Å)	9.95	10.095	10.195
V (Å ³)	1957.3	1981.9	2042.5

Several studies (Gilman 1998; Kuklja, Stefanovich, and Kunz 2000; Wu, Zhu, and Xiao 2014, 2013; Zhu et al. 2007) reported that electronic structure of energetic compounds has a significant influence on their structures and properties. Zhu et al. (2007) reported the relationship between band gap and sensitivity: A smaller band gap means an easier transferring of an electron from the valence bands to the conduction bands, and consequently, an external stimuli can more easily decompose the energetic material, leading to explosion. The band gap of ETT is 6.4 eV between valence and conduction bands, that is to say ETT is not sensitivity to explosion. The band structure reported in Figure 6 demonstrates that it is simple and appears to vary only in the width of the energy band.

It is found that the top of the valence bands (VBs) has large dispersion, whereas the bottom of the conduction bands (CBs) has a relatively small dispersion, shown in Figure 7. The lowest energy of CBs (6.4 eV) and highest energy (0.00 eV) of VBs are both localized at G point. The VBs between -20.0 and -15.0 eV are created by 2s states of N, O, and Cl mixing with small 2p states of C and Cl. The VBs between -15.0 and 0.0 eV are mostly attributed by 2p states of N, O, and Cl. The CBs between 0.0 and 10.0 eV are almost the contribution from O-2p and C-2p states hybridized with a small amount of N-2s, N-2p and Cl-2s, Cl-2p states.

Structure under high pressure

When energetic materials explode, the pressure can reach up to 30 GPa. Thus, it is necessary to investigate the band gap of the ETT under different pressures. The relaxed lattice constants of the ETT at various hydrostatic pressures (0–100 GPa) are shown in Figure 8. It can be seen from Figure 8 that the lattice parameters (a , b , c , and V) decrease along with the increase of pressure below 80 GPa. It is worth noting that b increases abnormally in the region between 80 and 100 GPa, indicating that the structural transformation may happen in the regions. Obviously, the lattice parameters decrease sharply below 40 GPa, implying that the unit cell can be easily compressed in this region. In the range of 0–40 GPa, the decreases of a , b , c , and V are 17.09%,

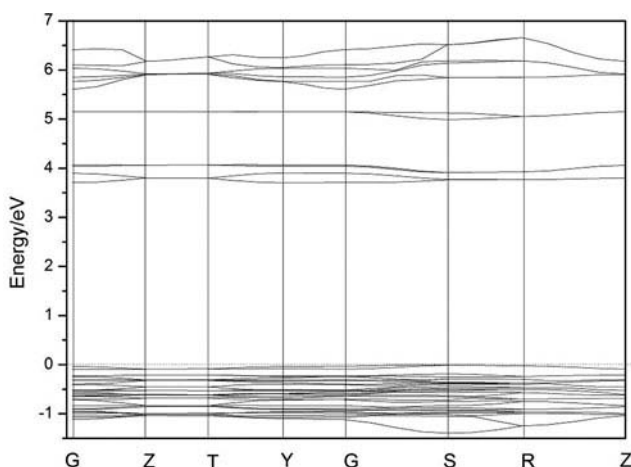


Figure 6. Energy band of ETT.

21.37%, 13.08%, and 46.27%, respectively, which are much more larger than 5.10%, 2.31%, 6.68%, and 14.02% in the range of 50–100 GPa. In the low-pressure region, the distance between the molecules is far, so the intermolecular repulsion is not large. Therefore, the crystal is easily compressed compared to the chemical bond. However, in the high-pressure region, the intermolecular repulsion is much larger, and the crystal is difficult to be compressed. Therefore, it is evident that the compressibility along three directions is different, which indicates that the compressibility of the crystal is anisotropic.

Electronic structure

Band gaps of the ETT at different pressures were also calculated as presented in Figure 9. Generally, the band gap decreases with the increasing pressure. In the region of 0–50 GPa, the band gap gradually increases from 6.4 to 6.503 eV due to the compression of the unit cell, leading to the increase of the charge overlap. From 60 to 100 GPa, band gap decreases suddenly, but at 80 GPa, the band gap increases a little. It is known that the smaller the band gap, the easier the electrons transfer from valence band to conduction band (Zhu et al. 2007). This implies that the ETT is more sensitive in the high-pressure region.

The calculated density of states (DOS) of the ETT is shown in Figure 10 with the Fermi level indicated by a dashed line. According to Figure 9, the character of the DOS can be summarized as follows: (1) with the increase in pressure, the peaks become smaller. When the pressure is 0, there are five main peaks in the DOS as discussed earlier, and in the high-pressure zone (80–100 GPa), only three main peaks are left. This is because more and more orbitals become hybridized under high pressure. (2) The top of VB and the bottom of the CB are mainly from p orbitals, indicating that the p orbitals play an important role in chemical reaction. In addition, the CBs shift to a lower energy region with the increasing pressure.

Hirshfeld surfaces

The Hirshfeld surfaces of the ETT were mapped over d_{norm} from -0.5 to 1.5 Å. As illustrated in Figure 11, red dots on the Hirshfeld surfaces indicate hydrogen bonding contacts. Weak interactions between Cl–O and N–O manifest in Hirshfeld surfaces are indicated as red areas. The 2D fingerprint plot of the ETT is shown in Figure 12, which indicates that the weak interactions are caused by H...O, O...O and C...C contacts. H...O and O...O intermolecular interactions contribute 34.8%

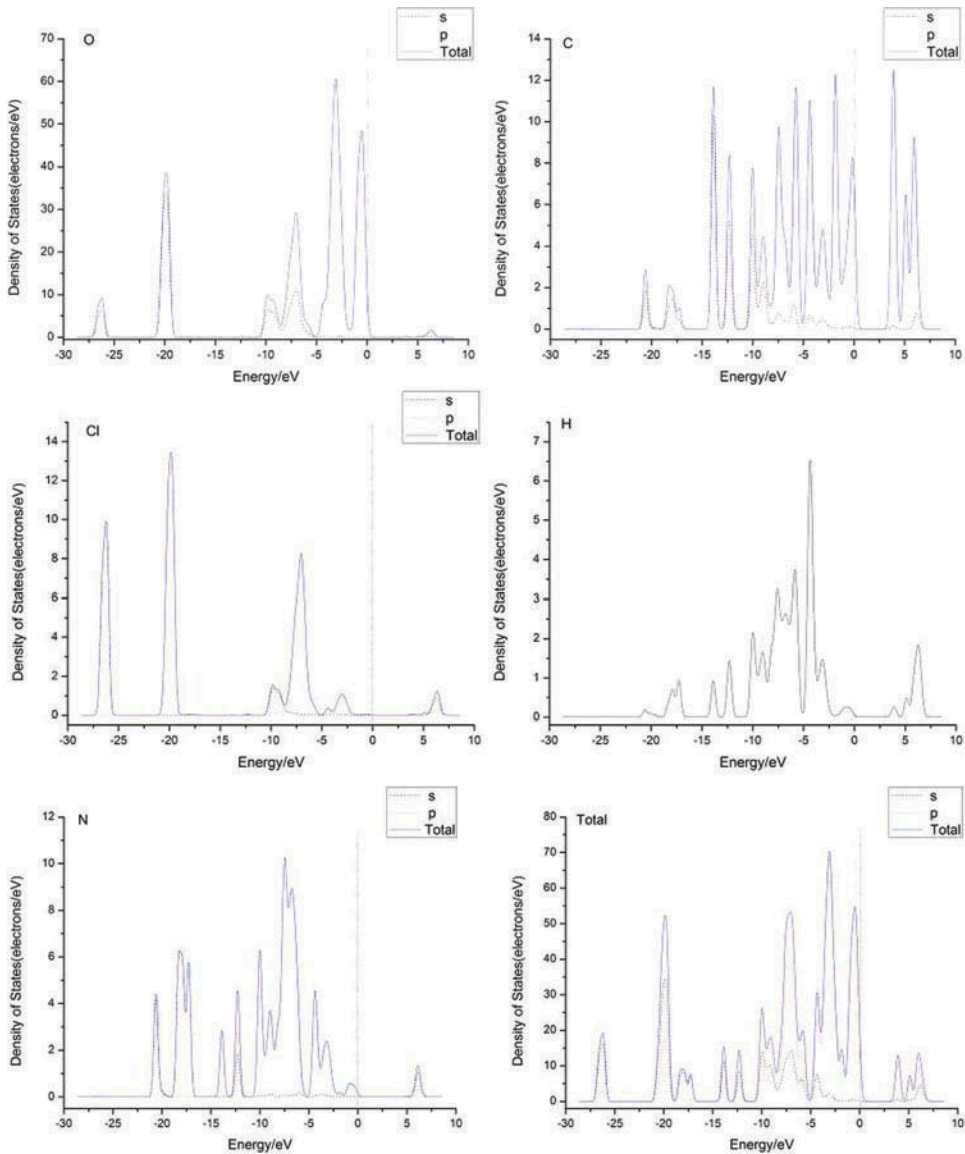


Figure 7. Total and partial density of states (DOS) of ETT.

and 19.0% to the total Hirshfeld surface, respectively, while C ... C interactions, appearing in the middle of the scattered points in the 2D fingerprint plot, contribute 7.3% to the total Hirshfeld surfaces. The perchlorate ions surround the crystal domains the intermolecular H ... O interactions which lead to the high population of H ... O interactions.

Trigger bond length of ETT

The explosive is triggered by a weak bond, which breaks preferentially with external stimuli, causing thermal decomposition or detonation. The change of bond length at different temperatures is shown in Table 6. According to Table 6, the bonds of Cl-O, C-N, and C-C changed a little with the increase in temperature, but the bond of N-H modified a lot. This indicates that N-H is sensitive to

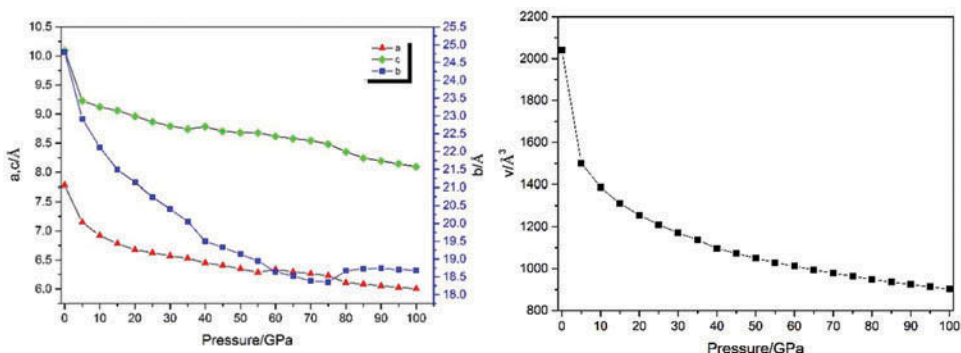


Figure 8. Lattice parameters under high pressure.

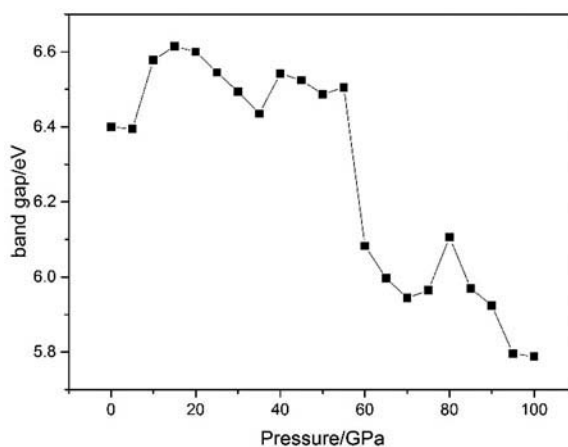


Figure 9. Band gap of ETT at different pressures.

temperature and works as the trigger bond. Based on a production trajectory, a molecular dynamic simulation gives the statistical bond distribution length shown in Figure 13. The average bond length (1.04203 Å) of N-H for ETT is close to the experimental value (1.03862 Å). The study from Xiao et al. (Zhu et al. 2010) showed that the molecules with maximum bond length were “activated,” and a lower impact sensitivity of energetic materials indicated shorter maximum bond lengths L_{max} . With the increasing temperature, the average bond lengths L_{ave} , as well as maximum bond lengths L_{max} , of all the models increase. That is to say, the variation in the trend of L_{max} reflects that the sensitivity increases with rising temperature.

Conclusions

In this work, a “one-pot” method was employed to synthesis a new kind of inorganic-organic co-crystal energetic material: ETT. The co-crystal displays a unique thermal behavior with a decomposition peak at 365 °C. In addition, the ETT exhibits a reduced impact sensitivity compared with its components and PETN. The detonation performance of the ETT is much better than that of RDX and TNT. The investigation of the crystal structure shows that there is a new kind of trigeminal-type hydrogen bond in the structure, H from amine could form three hydrogen bonds with O from three different perchlorates, which could form strong intermolecular and intramolecular hydrogen bonds to stabilize the co-crystal. A band structure analysis of the ETT showed that the top of VBs has a large dispersion, whereas the

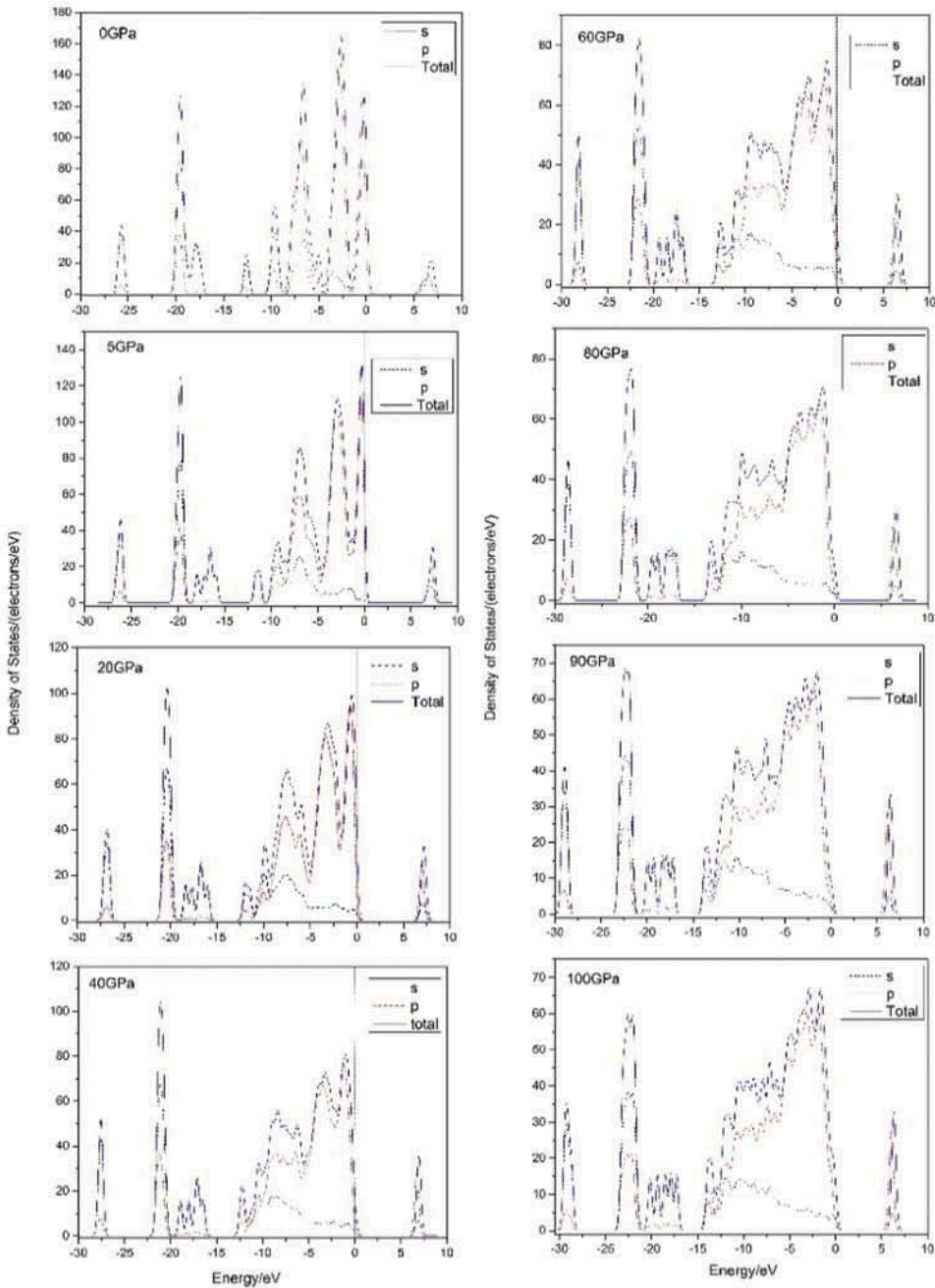


Figure 10. DOS of ETT at different pressures.

bottom of CBs has a relatively small dispersion. High pressure can change gradually lattice parameters and volume of the ETT. Under high pressure, hydrogen bonds become shorter, while the density increases, which could enhance the detonation performance. DOS analysis of the ETT at high pressure indicates that *p* orbitals play an important role in chemical reaction. The Hirshfeld surfaces analysis shows that H ... O and O ... O intermolecular interactions contribute 34.8% and 19.0% to the total Hirshfeld surface, making the intermolecular H ... O interactions dominant.

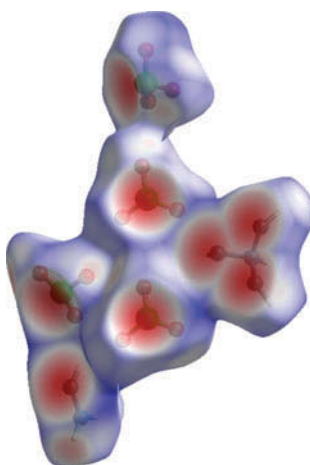


Figure 11. Hirshfeld surfaces mapped with d_{norm} for ETT.

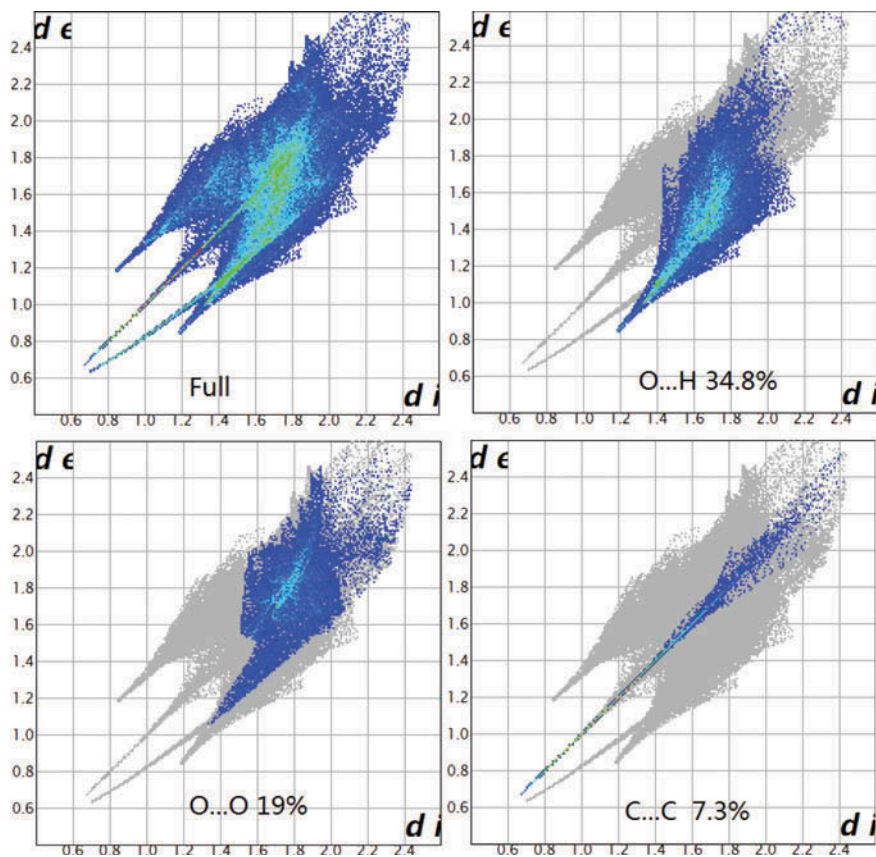
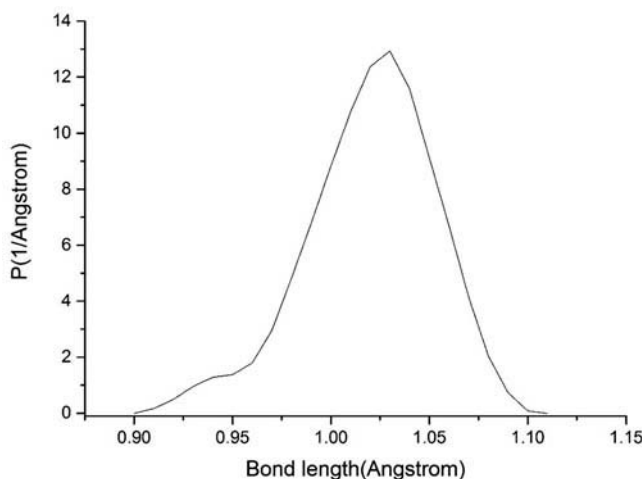


Figure 12. 2D fingerprint plots of ETT.

Table 6. Bond length of ETT at different temperatures.

Bond length (Å)		Temperature (K)						
		213	273	333	393	453	483	513
Cl-O	L _{ave}	1.58	1.58	1.58	1.58	1.59	1.59	1.59
	L _{max}	1.66	1.66	1.67	1.67	1.67	1.68	1.68
C-N	L _{ave}	1.47	1.47	1.47	1.47	1.47	1.48	1.48
	L _{max}	1.55	1.55	1.55	1.55	1.55	1.56	1.56
C-C	L _{ave}	1.53	1.53	1.53	1.53	1.53	1.53	1.53
	L _{max}	1.57	1.57	1.57	1.57	1.57	1.57	1.57
N-H	L _{ave}	1.01	1.04	1.04	1.06	1.07	1.07	1.08
	L _{max}	1.04	1.08	1.10	1.11	1.15	1.15	1.17

**Figure 13.** Bond length of N-H distribution at 333 K.

Funding

This research was supported by National Natural Science Fund of China (No.21436006, 21576136). P. Ma would like to thank the China Postdoctoral Science Foundation (grant no.2014M551579) and Postdoctoral of Jiangsu Province (grant no. 1401104C) for partial financial support.

References

- Anniyappan, M., S. H. Sonawane, S. J. Pawar, and A. K. Sikder. 2015. Thermal decomposition and kinetics of 2, 4-dinitroimidazole: An insensitive high explosive. *Thermochimica Acta* 614:93–99. doi:10.1016/j.tca.2015.05.027.
- Badgajar, D., M. Talawar, S. Asthana, and P. Mahulikar. 2008. Advances in science and technology of modern energetic materials: An overview. *Journal of Hazardous Materials* 151:289–305. doi:10.1016/j.jhazmat.2007.10.039.
- Bolton, O., and A. J. Matzger. 2011. Improved stability and smart-material functionality realized in an energetic cocrystal. *Angewandte Chemie International Edition* 50:8960–63. doi:10.1002/anie.v50.38.
- Bolton, O., L. R. Simke, P. F. Pagoria, and A. J. Matzger. 2012. High power explosive with good sensitivity: A 2: 1 cocrystal of CL-20: HMX. *Crystal Growth and Design* 12 (9):4311–14. doi:10.1021/cg3010882.
- Dippold, A. A., D. Izsák, and T. M. Klapötke. 2013. A Study of 5-(1, 2, 4-Triazol-C-yl) tetrazol-1-ols: Combining the benefits of different heterocycles for the design of energetic materials. *Chemistry—A European Journal* 19:12042–51. doi:10.1002/chem.201301339.
- Fischer, T. H., and J. Almlof. 1992. General methods for geometry and wave function optimization. *The Journal of Physical Chemistry* 96:9768–74. doi:10.1021/j100203a036.
- Ghule, V. D. 2013. Computational screening of nitrogen-rich energetic salts based on substituted triazine. *The Journal of Physical Chemistry C* 117:16840–49. doi:10.1021/jp405631c.
- Gilman, J. J. 1998. Fast, faster, and fastest cracks. *Philosophical Magazine Letters* 77:79–82. doi:10.1080/095008398178633.

- Guo, D., Q. An, S. V. Zybin, W. A. Goddard III, F. Huang, and B. Tang. 2015. The co-crystal of TNT/CL-20 leads to decreased sensitivity toward thermal decomposition from first principles based reactive molecular dynamics. *Journal of Materials Chemistry A* 3:5409–19. doi:10.1039/C4TA06858K.
- Guo, C., H. Zhang, X. Wang, J. Xu, Y. Liu, X. Liu, and J. Sun. 2013. Crystal structure and explosive performance of a new CL-20/caprolactam cocrystal. *Journal of Molecular Structure* 1048:267–73. doi:10.1016/j.molstruc.2013.05.025.
- Kuklja, M. M., E. V. Stefanovich, and A. B. Kunz. 2000. An excitonic mechanism of detonation initiation in explosives. *The Journal of Chemical Physics* 112:3417–23. doi:10.1063/1.480922.
- Landenberger K B, Bolton O, Matzger A J. 2013. Two isostructural explosive cocrystals with significantly different thermodynamic stabilities. *Angewandte Chemie International Edition*, 2013, 52: 6468–6471.
- Landenberger, K. B., and A. J. Matzger. 2010. Cocrystal engineering of a prototype energetic material: Supramolecular chemistry of 2, 4, 6-trinitrotoluene. *Crystal Growth and Design* 10:5341–47. doi:10.1021/cg101300n.
- Landenberger, K. B., and A. J. Matzger. 2012. Cocrystals of 1, 3, 5, 7-Tetranitro-1, 3, 5, 7-tetrazacyclooctane (HMX). *Crystal Growth and Design* 12:3603–09. doi:10.1021/cg3004245.
- Lin, H., P. Y. Chen, S. G. Zhu, L. Zhang, X. H. Peng, and H. Z. Li. 2013a. Computational study of pyrazine-based derivatives and their N-oxides as high energy materials. *Journal of Physical Organic Chemistry* 26:484–91. doi:10.1002/poc.3113.
- Lin, H., P. Y. Chen, S. G. Zhu, L. Zhang, X. H. Peng, K. Li, and H. Z. Li. 2013b. Theoretical studies on the thermodynamic properties, densities, detonation properties, and pyrolysis mechanisms of trinitromethyl-substituted aminotetrazole compounds. *Journal of Molecular Modeling* 19:2413–22. doi:10.1007/s00894-013-1783-2.
- Lin, H., S. G. Zhu, H. Z. Li, and X. H. Peng. 2013. Synthesis, characterization, AIM and NBO analysis of HMX/DMI cocrystal explosive. *Journal of Molecular Structure* 1048:339–48. doi:10.1016/j.molstruc.2013.06.013.
- Lin, H., S. G. Zhu, L. Zhang, X. H. Peng, P. Y. Chen, and H. Z. Li. 2013a. Intermolecular interactions, thermodynamic properties, crystal structure, and detonation performance of HMX/NTO cocrystal explosive. *International Journal of Quantum Chemistry* 113:1591–99. doi:10.1002/qua.24369.
- Lin, H., S. G. Zhu, L. Zhang, X. H. Peng, P. Y. Chen, and H. Z. Li. 2013b. Theoretical investigation of a novel high density cage compound 4, 8, 11, 14, 15-pentanitro-2, 6, 9, 13-tetraoxa-4, 8, 11, 14, 15-pentazaheptacyclo [5.5. 1.13, 11. 15, 9] pentadecane. *Journal of Molecular Modeling* 19:1019–26. doi:10.1007/s00894-012-1629-3.
- Lin, H., S. G. Zhu, H. Z. Li, and X. H. Peng. 2013c. Synthesis, characterization, AIM and NBO analysis of HMX/DMI cocrystal explosive. *Journal of Molecular Structure* 1048:339–48. doi:10.1016/j.molstruc.2013.06.013.
- Lin, H., S. G. Zhu, L. Zhang, X. H. Peng, P. Y. Chen, and H. Z. Li. 2013d. Intermolecular interactions, thermodynamic properties, crystal structure, and detonation performance of HMX/NTO cocrystal explosive. *International Journal of Quantum Chemistry* 113:1591–99. doi:10.1002/qua.24369.
- Lin, H., S. G. Zhu, L. Zhang, X. H. Peng, P. Y. Chen, and H. Z. Li. 2013e. Theoretical investigation of a novel high density cage compound 4, 8, 11, 14, 15-pentanitro-2, 6, 9, 13-tetraoxa-4, 8, 11, 14, 15-pentazaheptacyclo [5.5. 1.13,11. 15, 9] pentadecane. *Journal of Molecular Modeling* 19:1019–26. doi:10.1007/s00894-012-1629-3.
- Millar, D. I., H. E. Maynard-Casely, D. R. Allan, A. S. Cumming, A. R. Lennie, A. J. Mackay, and C. R. Pulham. 2012. Crystal engineering of energetic materials: Co-crystals of CL-20. *CrystEngComm* 14:3742–49. doi:10.1039/c2ce05796d.
- Perdew, J. P., K. Burke, and M. Ernzerhof. 1996. Generalized gradient approximation made simple. *Physical Review Letters* 77:3865–68. doi:10.1103/PhysRevLett.77.3865.
- Remenar, J. F., S. L. Morissette, M. L. Peterson, B. Moulton, J. M. MacPhee, H. R. Guzmán, and Ö. Almarsson. 2003. Crystal engineering of novel cocrystals of a triazole drug with 1, 4-dicarboxylic acids. *Journal of the American Chemical Society* 125:8456–57. doi:10.1021/ja035776p.
- Rice, B. M., J. J. Hare, and E. F. C. Byrd. 2007. Accurate predictions of crystal densities using quantum mechanical molecular volumes. *The Journal of Physical Chemistry A* 111:10874–79. doi:10.1021/jp073117j.
- Segall, M. D., P. J. Lindan, M. A. Probert, C. J. Pickard, P. J. Hasnip, S. J. Clark, and M. C. Payne. 2002. First-principles simulation: Ideas, illustrations and the CASTEP code. *Journal of Physics Condensed Matter* 14:2717. doi:10.1088/0953-8984/14/11/301.
- Shen, J. P., X. H. Duan, Q. P. Luo, Y. Zhou, Q. Bao, Y. J. Ma, and C. H. Pei. 2011. Preparation and characterization of a novel cocrystal explosive. *Crystal Growth and Design* 11:1759–65. doi:10.1021/cg1017032.
- Sikder, A. K., and N. Sikder. 2004. A review of advanced high performance, insensitive and thermally stable energetic materials emerging for military and space applications. *Journal of Hazardous Materials* 112:1–15. doi:10.1016/j.jhazmat.2004.04.003.
- van der Heijden, A. E., R. H. Bouma, and A. C. van der Steen. 2004. Physicochemical parameters of nitramines influencing shock sensitivity. *Propellants, Explosives, Pyrotechnics* 29:304–13. doi:10.1002/prep.200400058.
- Vanderbilt, D. 1990. Soft self-consistent pseudopotentials in a generalized eigenvalue formalism. *Physical Review B* 41:7892–95. doi:10.1103/PhysRevB.41.7892.
- Weyna, D. R., T. Shattock, P. Vishweshwar, and M. J. Zaworotko. 2009. Synthesis and structural characterization of cocrystals and pharmaceutical cocrystals: Mechanochemistry vs slow evaporation from solution. *Crystal Growth and Design* 9:1106–23. doi:10.1021/cg800936d.

- Wolff, S. K., D. J. Grimwood, J. J. McKinnon, M. J. Turner, D. Jayatilaka, and M. A. Spackman. 2012. *Crystal Explorer*. Australia: The University of Western Australia.
- Wu, Q., W. Zhu, and H. Xiao. 2013. Structural transformations and absorption properties of crystalline 7-amino-6-nitrobenzodifuroxan under high pressures. *The Journal of Physical Chemistry C* 117:16830–39. doi:10.1021/jp405591j.
- Wu, Q., W. Zhu, and H. Xiao. 2014. Pressure-induced hydrogen transfer and polymerization in crystalline furoxan. *RSC Advances* 4:15995–6004. doi:10.1039/C3RA47747A.
- Xue, H., Y. Gao, B. Twamley, and J. N. M. Shreeve. 2005. New energetic salts based on nitrogen-containing heterocycles. *Chemistry of Materials* 17:191–98. doi:10.1021/cm048864x.
- Yin, P., D. A. Parrish, and J. N. M. Shreeve. 2015. Energetic multifunctionalized nitraminopyrazoles and their ionic derivatives: Ternary hydrogen-bond induced high energy density materials. *Journal of the American Chemical Society* 137:4778–86. doi:10.1021/jacs.5b00714.
- Zhang, J., and J. N. M. Shreeve. 2014. 3, 3'-Dinitroamino-4, 4'-azoxyfuroxan and its derivatives: An assembly of diverse N–O building blocks for high-performance energetic materials. *Journal of the American Chemical Society* 136:4437–45. doi:10.1021/ja501176q.
- Zhang, J., and J. M. Shreeve. 2016. Time for Pairing: Cocrystals as Advanced Energetic Materials. *CrystEngComm* 18:6124–33. doi:10.1039/C6CE01239F.
- Zhang C, Cao Y, Li H, et al. 2013. Toward low-sensitive and high-energetic cocrystal I: evaluation of the power and the safety of observed energetic cocrystals. *CrystEngComm*, 15: 4003–4014.
- Zhang, C., Z. Yang, X. Zhou, C. Zhang, Y. Ma, J. Xu, and H. Li. 2014. Evident hydrogen bonded chains building CL-20-based cocrystals. *Crystal Growth and Design* 14:3923–28. doi:10.1021/cg500796r.
- Zhu, W., and H. Xiao. 2010. First-principles band gap criterion for impact sensitivity of energetic crystals: A review. *Structural Chemistry* 21:657–65. doi:10.1007/s11224-010-9596-8.
- Zhu, W., J. Xiao, G. Ji, F. Zhao, and H. Xiao. 2007. First-principles study of the four polymorphs of crystalline octahydro-1, 3, 5, 7-tetranitro-1, 3, 5, 7-tetrazocine. *The Journal of Physical Chemistry B* 111:12715–22. doi:10.1021/jp075056v.